New Consideration of Non-Metallic Inclusions Calculating Local Tooth Root Load Carrying Capacity of High-Strength, High-Quality Steel Gears

Daniel Fuchs, Stefan Schurer, Thomas Tobie and Karsten Stahl

Demands for higher performance have caused a need for improved component characteristics, e.g. — through surface strengthening of gears and increased cleanliness of gear steels. Unfortunately, a resultant drawback is that cracks in such high-strength gears are more often initiated in the material matrix at non-metallic inclusions and not at the surface. In standardized calculation methods, the degree of cleanliness of steels is not yet directly correlated to the tooth root load carrying capacity. This paper considers the effects of non-metallic inclusions in the steel matrix on the tooth root strength based on the theoretical approach of Murakami.

Nomenclature

Symbol	Unit	Parameter
HV	HV	Vickers hardness of the steel matrix
K	MPa $\sqrt{m}$	stress intensity factor
K_A	–	application factor
K_v	–	dynamic factor
$K_{F\beta}$	–	face load factor for tooth root stress
$K_{F\alpha}$	–	transverse load factor for tooth root stress
M	–	mean stress sensitivity
M_E	–	residual stress sensitivity
m_n	mm	normal module
$\sqrt{area}$	m	square root of a defect area projected onto a plane perpendicular to the applied stress
σ_A	N/mm^2	local fatigue strength
σ_F	N/mm^2	maximum tooth root stress at the surface
σ_{F0}	N/mm^2	nominal tooth root stress at the surface
$\sigma_{inclusion}$	N/mm^2	local load induced stress at the depth of the non–metallic inclusion
σ_m	N/mm^2	local mean stress
σ_{RS}	N/mm^2	residual stress
σ_W	N/mm^2	local bending fatigue strength
$\frac{\sigma_{inclusion}}{\sigma_A}$	–	local material strength ratio

The trend towards higher performance requirements is becoming ever more important for gear manufacturers. According to the current state of knowledge, there are two common approaches for increasing the power density: either to build smaller gearboxes with equal transmittable power or to increase the transmittable power without changing the dimensions. Consequently, approaches such as the surface strengthening of gears have become more important in the last decade. In addition, a lot of effort has been invested by steel manufacturers in improving material properties, such as an increased cleanliness of the steel or use of new alloy combinations.

Unfortunately, the approaches are not without drawbacks, such as cracks in high-strength gears that are now more often initiated in the material matrix and not at the surface — even after years of operation. If such damage mechanisms occur during operating, they result in high costs and are a major problem for both gear manufacturers and operators.

Most of these sub-surface-initiated cracks occur at non-metallic inclusions; therefore the degree of cleanliness of the steel used is highly important. In standardized calculation methods, e.g. — ISO 6336-3 (Ref. 15) or DIN 3990-3 (Ref. 17) — the degree of cleanliness of steels has not yet been directly correlated to the tooth root (bending) load carrying capacity. Therefore, it is not yet possible to determine the actual bending strength of high-quality gears.

The theoretical approach of Murakami (Ref. 2) provides a first basis for determining the load carrying capacity for component parts with non-metallic inclusions. The research conducted for this paper is based on this approach and on extensive experimental results obtained on FZG back-to-back gear test rigs and pulsator test rigs.

It can be shown that the model of Murakami can be adapted for gears. The developed model is in good correlation with the experimental results. This paper shows how these results allow a consideration of the effects of non-metallic inclusions in the matrix of gear steels on the tooth root bending strength.

Basics

The cracking mechanism of shotpeened gears is different from that of un-peened gears. Due to high beneficial, compressive residual stresses in the area near to the surface, the critical stress for crack initiation lies below the surface. In the event of a non-metallic inclusion in this area, the stress is increased even more due to local stress step-up.

A typical crack area caused by a crack initiation at a non-metallic inclusion is illustrated (Fig. 1). This kind of crack mechanism is known as "fish-eye-failure" because of the typical appearance. Typically, a non-metallic inclusion is surrounded by an optically dark area (ODA) — also known as granular bright face (GBF) or fine granular area (FGA). As soon as the fish-eye reaches the surface, the crack propagates rapidly through the

rest of the material and the part fails.

Non-metallic inclusions in gear steels. In gear steels such as 16MnCr5 and 18CrNiMo7-6, the common non-metallic inclusions are manganese sulphides in the case of MnCr-alloyed steels and aluminum oxides in the case of CrNiMo-alloyed steels. The shape of manganese sulphide inclusions is primarily oblong, while the shape of aluminum oxide inclusions is primarily spherical (Refs. 7–8).

The cracks are primarily initiated at non-metallic inclusions, so the fewer the number and the smaller the inclusions, the lower is the probability of crack initiation at such inclusions. In the case of MnCr-alloyed steels, the cracks are primarily initiated at manganese sulphide inclusions (Fig. 2a); in the case of CrNiMo-alloyed steels the initiators primarily occur at aluminum oxide inclusions (Figs. 2b and 2c) (Refs. 7–8).

Test rigs. To substantiate the model approach, extensive experimental tests were performed on FZG back-to-back test rigs with a center distance of $a = 91.5$ mm (Ref. 14) and on pulsator test rigs (Ref. 8). The FZG back-to-back gear test rig utilizes a recirculating power loop principle (Fig. 3a) to supply a fixed torque to a pair of test gears in the test gearbox. A three-phase asynchronous electric motor drives the test rig at a constant speed. Test pinion and test gear are mounted on two parallel shafts that are connected to a drive gear stage with the same gear ratio. The shaft of the test pinion consists of two separate parts connected by a load clutch. A defined static torque is applied by twisting the load clutch. The torque can be controlled indirectly at the torque-measuring clutch by twisting the torsion shaft. (Ref. 10)

On the pulsator test rig the test gear is fixed over, for example, four teeth between two clamps (Fig. 3b); a defined mid-load is applied by the mid-load actuator. The variable exciting mass, pole spring, and upper clamp are excited by the exciting magnet to test the test gear. To obtain a uniform load distribution for all tests, the clamping was always symmetrical and fine flank angle deviations were adjusted. (Ref. 19)

Test gears. The test gears were made of the steel grades 16MnCr5, 20MnCr5 and 18CrNiMo7-6, supplied by various steel manufacturers with a higher degree of cleanliness than common grades. The cast processes, ingot, and continuous casting were used in combination with metallurgic processes such as open-melted or electro-slag re-melt (ESR). A few special grades, such as aluminum-free, complete the test matrix. A total of 17 different steel variants were tested in three gear sizes.

The test gear sizes used were $m_n = 1.5$ mm, $m_n = 5$ mm and $m_n = 10$ mm; an excerpt of the gear data is listed in Table 1. All three test gear sizes were tested on the pulsator test rig. Tests on the FZG back-to-back test rig were performed with module $m_n = 1.5$ mm gears only.
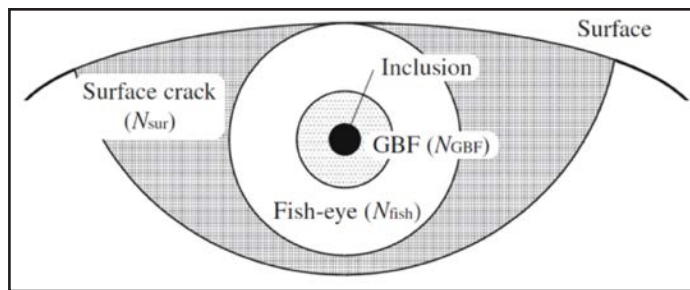

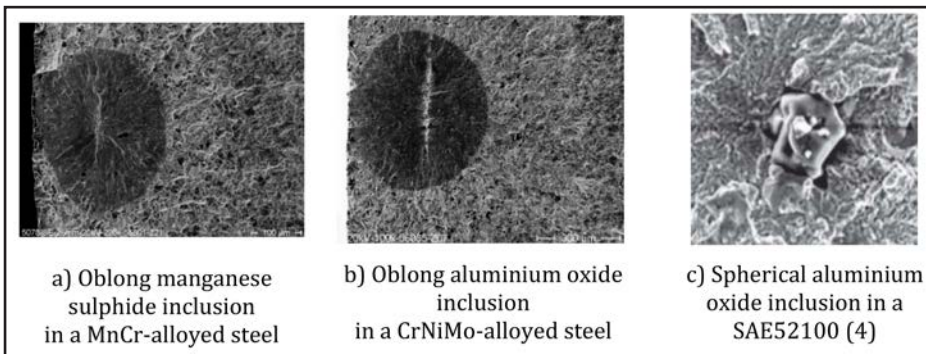**Figure 1   Schematic illustration of sub-surface crack growth around a non-metallic inclusion (Ref. 9).**

a) Oblong manganese sulphide inclusion in a MnCr-alloyed steel

b) Oblong aluminium oxide inclusion in a CrNiMo-alloyed steel

c) Spherical aluminium oxide inclusion in a SAE52100 (4)

Figure 2   Typical non-metallic inclusions in gear steels.

a) FZG back-to-back test rig with a centre distance of $a = 91.5$ mm (14)
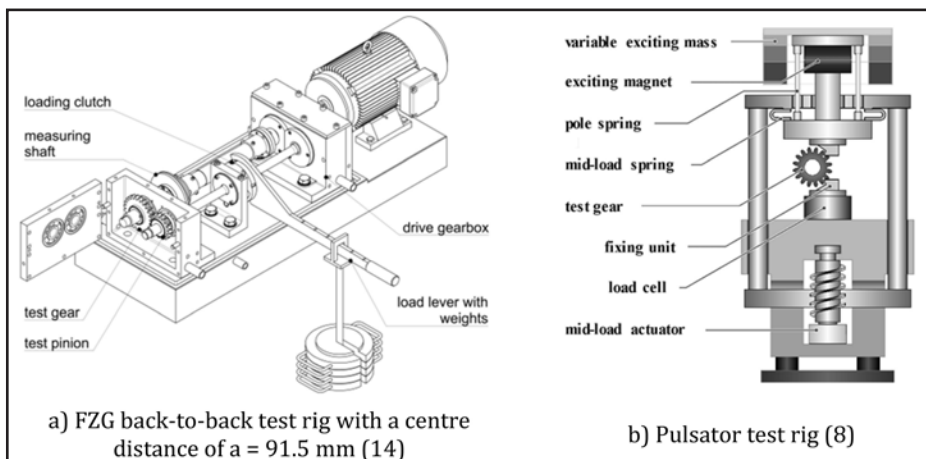
b) Pulsator test rig (8)

Figure 3   Test rigs at the Gear Research Centre (FZG) at the Technical University of Munich (TUM).

Table 1 Excerpt of the test gear data (Refs. 7–8)			
normal module in mm	$m_n = 1.5$	$m_n = 5$	$m_n = 10$
test rig	FZG back-to-back test rig	Pulsator test rig	
center distance	91.5 mm	–	
tooth number z_1/z_2	59 / 61	24	
gear width	8	30	
standard pressure angle	20°		
helix angle	0°		

A scanning electron microscope (SEM) and an energy-dispersive X-ray spectrometer (EDX) were used to analyze the non-metallic inclusions in the fractured surfaces. Amongst other things, the area and distance from the surface of the non-metallic inclusions were analyzed (Fig. 4).

Measured distances from the surface were between 77 µm and 1,377 µm across all the gear sizes tested. The average for the gears with module $m_n = 1.5$ mm was 138 µm; for module $m_n = 5$ mm 227 µm; and for module $m_n = 10$ mm 1,067 µm. In the current research all of the non-metallic inclusions that were responsible for causing a failure were located within the case hardened layer (Fig. 5).

The parameter $\sqrt{area}$ used in the theoretical approach of Murakami (Ref. 2) is the square root of a defect area projected onto a plane perpendicular to the applied stress (Fig. 6). It shows an internal crack in the x–y plane of an infinite solid that is subject to a uniform remote tensile stress σ_0 in the z-direction.

Model Approach

The local material strength ratio $\sigma_{inclusion}/\sigma_A$ — which defines theoretically whether crack initiation occurs or not — is the ratio of the local stress at the non-metallic inclusion $\sigma_{inclusion}$ to the local bending fatigue strength σ_A (Fig. 7). However, certain input factors are necessary for calculation and these are presented below.
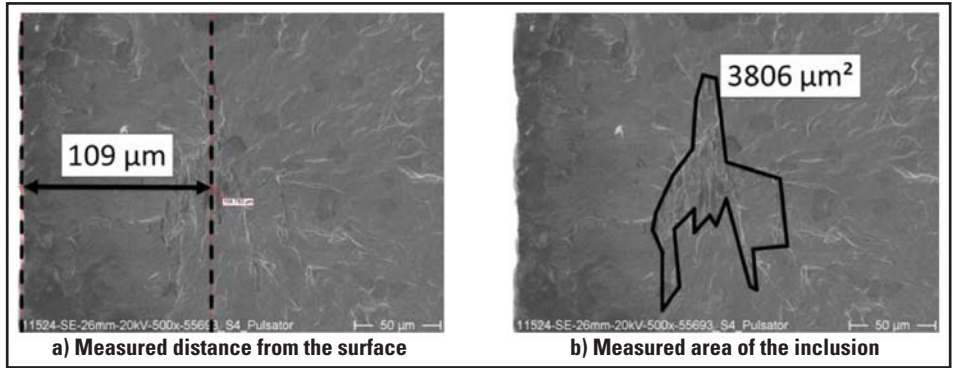

a) Measured distance from the surface   **b) Measured area of the inclusion**

Figure 4   Typical analysis of the characteristics of a manganese-sulphide non-metallic inclusion.
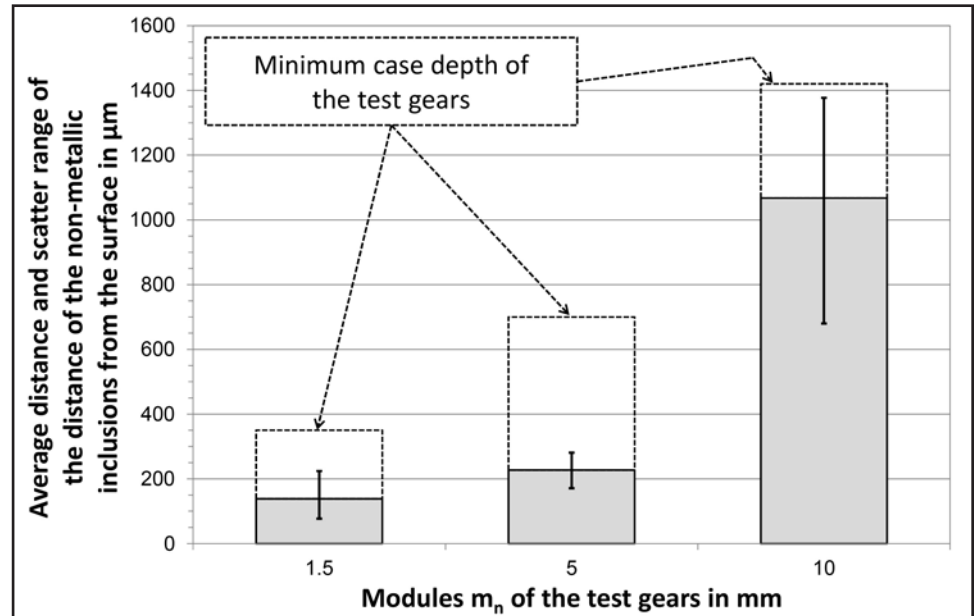

Figure 5   Average distance and scatter range of the distance of the non-metallic inclusions from the surface and comparison with the minimum case depth of the three test gear sizes.
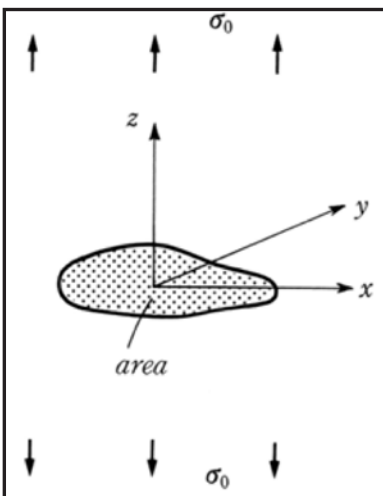

Figure 6   Arbitrarily shaped 3D internal crack ("area" = area of crack) (Ref. 2).
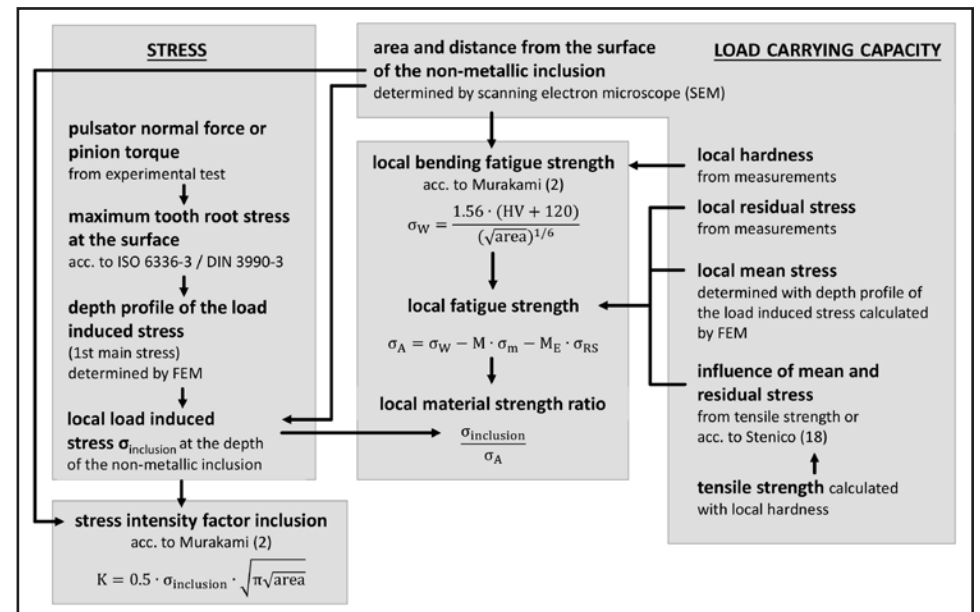

Figure 7   Schematic diagram of the procedure of the calculation study (Ref. 7).

Determination of local stress at the non-metallic inclusion: $\sigma_{inclusion}$. A number of steps are required to determine local stress at the non-metallic inclusion $\sigma_{inclusion}$. First, in accordance with ISO 6336-3 (Ref. 15) or DIN 3990-3 (Ref. 17), the maximum tooth root stress at the surface σ_F must be calculated according to Equation 1, based on the pulsator normal force or pinion torque.

$$\sigma_F = \sigma_{F0} \cdot K_A \cdot K_V \cdot K_{F\beta} \cdot K_{F\alpha} \qquad (1)$$

Next, the depth profile of the load stress (1st main normal stress), determined using the finite element method (FEM) (Fig. 8), is required to convert the value at the surface to a value at the specific local distance from the surface of the non-metallic inclusion. The local distance is determined by examination of the fractured surface of the broken tooth using the scanning electron microscope (SEM). These input factors form the local stress at the non-metallic inclusion.

Determination of the local fatigue strength: σ_A. The local bending fatigue strength σ_W according to Murakami must be determined based on Equation 2, using the measured area of the non-metallic inclusion $\sqrt{area}$ and the local Vickers hardness HV — which are both determined by measurement.

$$\sigma_W = \frac{1.56 \cdot (HV + 120)}{(\sqrt{area})^{1/6}} \qquad (2)$$

By considering the local mean stress σ_m and residual stress σ_{RS} the local bending fatigue strength σ_W can be reassessed using the Goodman approach to form an equivalent local fatigue strength σ_A (Eq. 3). To do so, the local hardness and the local residual stress must be measured. Based on a depth profile of the load-induced specific local stress determined using FEM, the local mean stress σ_m is calculated. The influence of the mean and residual stress is evaluated by the tensile strength respectively, according to Stenico (Ref. 18); the tensile strength is calculated using the local hardness.

$$\sigma_A = \sigma_W - M \cdot \sigma_m - M_E \cdot \sigma_{RS} \qquad (3)$$

On the basis of comparable case hardness and core hardness of the steel used and previous investigations (Refs. 12, 18) the parameters $M = 0.3$ and $M_E = 0.2$ were used.

Results

As described in the previous section, the non-metallic inclusions were investigated and measured using a SEM and the stress intensity factor K calculated according to Equation 4. The stress intensity factor K is plotted against the number of load cycles N until failure (Fig. 9).

$$K = 0.5 \cdot \sigma_{inclusion} \cdot \sqrt{\pi \cdot \sqrt{area}} \qquad (4)$$

The results show that with decreasing local stress step-up, i.e. a smaller inclusion size and/or local stress, the number of load cycles N until tooth root failure increases. Crack propagation is slower at greater distances from the surface of the non-metallic inclusion, or if the local stress is lower and therefore the high cycle fatigue lifetime increases.

Based on the extensive experimental data, an asymptotic trend and consequently a limiting threshold of the stress intensity factor K are to be expected. The results are also in agreement with other research (Refs. 2, 3, 6 and 18). The aluminum-free variant S3 differs from the other variants. This can be explained by the specific production route, as well as the
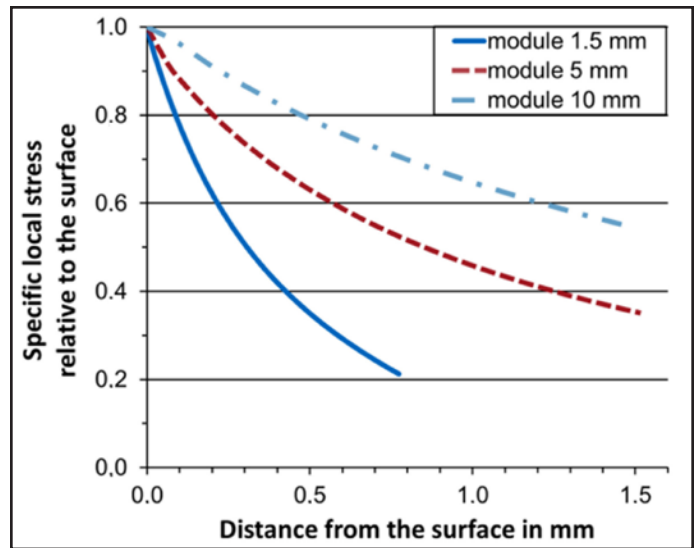

Figure 8 Depth profile of the load-induced specific local tooth root stress relative to the surface determined using the finite element method (1st main stress) (Ref. 7).
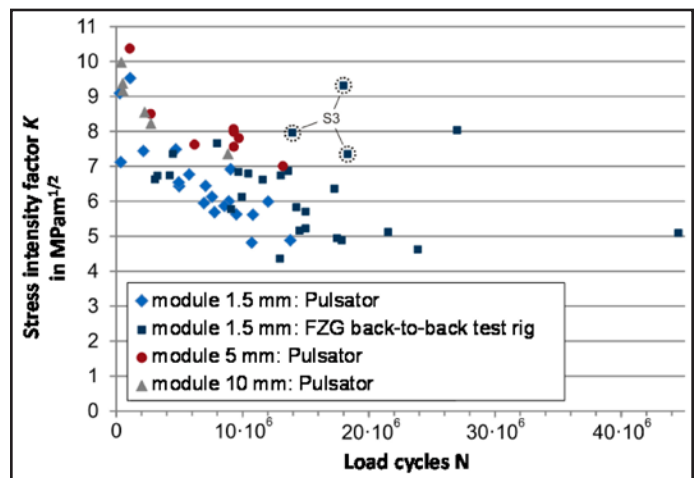

Figure 9 Estimation of the local stress intensity factor K according to Murakami (Ref. 2) plotted against the experimentally determined number of load cycles N until tooth root failure (Ref. 7).
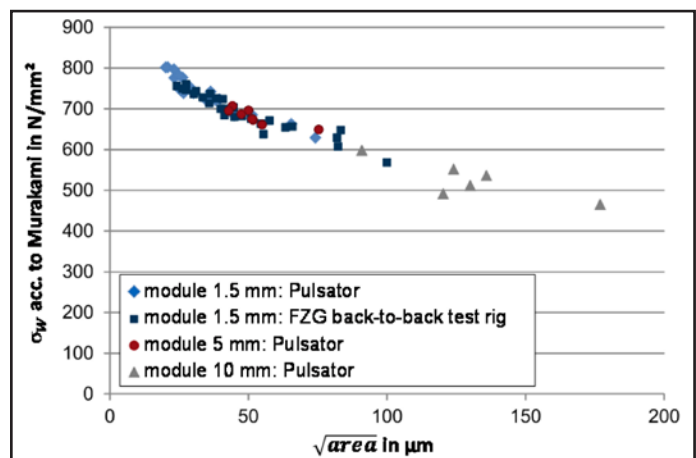

Figure 10 Estimated local bending fatigue strength σ_W taking into consideration of non-metallic inclusions according to Murakami (Ref. 2) for the experimentally performed tooth root load carrying capacity tests (Ref. 7).

special heat treatment.

According to Equation 2, a local bending fatigue strength σ_w for each determined failure can be estimated by taking into consideration the hardness depth profile and the local hardness near the non-metallic inclusion (Fig 10). The results indicate that with increasing inclusion size ($\sqrt{area}$), the local bending fatigue strength σ_W decreases in agreement with Murakami (Ref. 2).

An estimation of the local fatigue strength σ_A according to Equation 3 is possible based on the approach of Macherauch and Wohlfahrt ((Refs. 1, 11) according to (Ref. 6)), taking into consideration the existing mean stress and residual stress. The local material strength ratio $\sigma_{inclusion}/\sigma_A$ is plotted against the number of load cycles N until failure in Figure 11.
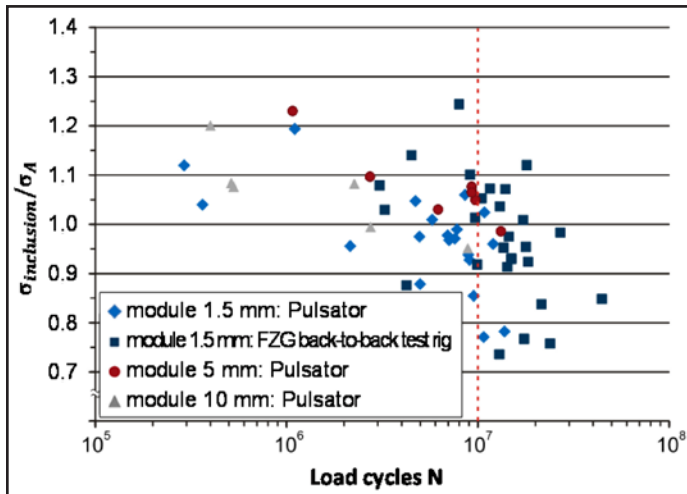

Figure 11 Local material strength ratio $\sigma_{inclusion}/\sigma_A$ plotted against the number of load cycles N until failure; load cycle limit of 10^7 according to Murakami (Refs. 2 and 7).

Most of the tests with load cycles below 10^7 comply with the common knowledge of the strength of materials and the model approach according to Murakami (Ref. 2). A crack initiation can occur when the local material strength ratio $\sigma_{inclusion}/\sigma_A$ is greater than 1. Almost all data points for $N < 10^7$ are in the range 1.0 ± 0.1. Only when the number of load cycles is greater than 10^7 does an increased number of test points fall outside this range that is below 0.9. However, it should be noted that the model used according to Murakami firstly only has a test accuracy of $\pm 10\%$ and is only valid up to 10^7 load cycles. According to Murakami, the optically dark area (ODA) must also be considered for higher numbers of load cycles (Ref. 5).

The results show that, in general, the model approach developed by Murakami (Ref. 2) can be applied to high-strength gears and that a direct correlation between the tooth root load carrying capacity and the degree of cleanliness of high-strength gears exists.

Conclusion

In modern engineering, surface strengthening of gears and increased cleanliness of gear steels have become more important. However, a resulting drawback is that cracks initiate more frequently at non-metallic inclusions, and not at the surface. In standardized calculation methods such as ISO 6336-3 (Ref. 15) or DIN 3990-3 (Ref. 17), the degree of cleanliness of gear steels is not currently directly correlated to the tooth root load carrying capacity.

It can be shown that, subject to a few restrictions, an approach for correlating between the cleanliness of gear steels and the resulting tooth root load carrying capacity based on the theoretical approach of Murakami (Ref. 2) is now possible. The results of the current research work show good agreement with the research work of Murakami. However, validation of the scatter range would be beneficial. The model approach for Murakami for $N > 10^7$ is basically applicable to gears; however, further research work is necessary. ⚙

References

1. Macherauch, E. and H. Wohlfahrt. Eigenspannungen und Ermüdung. Ermüdungsverhalten metallischer Werkstoffe (DGM-Informationsges.), pp. 237–83, 1985.
2. Murakami, Y. *Metal Fatigue — Effects of Small Defects and Non-Metallic Inclusions.* Elsevier, Amsterdam, 1ST Ed., 2002.
3. Murakami, Y. and M. Endo. "Effects of Defects, Inclusions and Inhomogeneities on Fatigue Strength," *International Journal of Fatigue* 16. Vol: 3, pp. 163–82, 1994.
4. Murakami, Y., H. Matsunaga and A. Abyazi, et al. "Defect Size Dependence on Threshold Stress Intensity for High-Strength Steel with Internal Hydrogen," *Fatigue Fracture of Engineering Materials and Structures* 36, Vol: 9, pp. 836–50, 2013.
5. Murakami, Y. and Y. Yamashita. "Prediction of Life and Scatter of Fatigue Failure Originated at Nonmetallic Inclusions," *Procedia Engineering* 74, pp. 6–11, 2014.
6. Radaj, D. and M. Vormwald. *Ermüdungsfestigkeit — Grundlagen für Ingenieure,* Springer, Berlin [u.a.], 2007.
7. Schurer, S. Einfluss Nichtmetallischer Einschlüsse in hochreinen Werkstoffen auf die Zahnfußtragfähigkeit. Dissertation, Technische Universität München.
8. Schurer, S., T. Tobie and K. Stahl. "Späte Zahnfußbrüche/Reinheitsgrad — Tragfähigkeitsgewinn im Zahnfuß durch hochreine Stähle," FVA-Nr. 293 III, Forschungsvereinigung Antriebstechnik e.V. (FVA), Frankfurt, 2015.
9. Shiozawa, K., M. Murai and Y. Shimatani, et al. Transition of Fatigue Failure Mode of Ni–Cr–Mo Low-Alloy Steel in Very High Cycle Regime, *International Journal of Fatigue* 32. Vol: 3, pp. 541–50, 2010.
10. Weber, C., T. Tobie and K. Stahl. "Investigation on the Flank Surface Durability of Gears with Increased Pressure angle — Investigation on the Flank Surface Durability of Gears with Increased Pressure Angle," Springer Berlin Heidelberg, Berlin/Heidelberg.
11. Wohlfahrt, H. "Einfluß von Mittelspannungen und Eigenspannungen auf die Dauerfestigkeit," *VDI-Berichte,* Vol: 661, pp. 99–127, 1988.
12. Bretl, N. "Einflüsse auf die Zahnfußtragfähigkeit einsatzgehärteter Zahnräder im Bereich hoher Lastspielzahlen," Dissertation, Technische Universität München, 2010.
13. Bretl, N. T., T. Tobie and B.-R. Höhn. Späte Zahnfußbrüche — Zahnfußbruch mit Rissausgang unter der Oberfläche an einsatzgehärteten Zahnrädern," FVA-Nr. 293 II, Forschungsvereinigung Antriebstechnik e.V. (FVA), Frankfurt, 2008.
14. DIN ISO 14635-1:2006. FZG-Prüfverfahren A/8, 3/90 zur Bestimmung der relativen Fresstragfähigkeit von Schmierölen, 2006.
15. ISO 6336-3:2006. Calculation of Load Capacity of Spur and Helical Gears — Part 3: Calculation of Tooth Bending Strength, 2006.
16. Löwisch, G. "Zuordnung von Werkstoffkennwerten zu Bauteileigenschaften von einsatzgehärteten und carbonitrierten Zahnrädern," Forschungsvereinigung Antriebstechnik e.V. (FVA), Frankfurt, 1994.
17. DIN 3990-3:1987. Tragfähigkeitsberechnung von Stirnrädern; Berechnung der Zahnfußtragfähigkeit, 1987.
18. Stenico, A. "Werkstoffmechanische Untersuchungen zur Zahnfußtragfähigkeit einsatzgehärteter Zahnräder," Dissertation, Technische Universität München, 2007.
19. Dobler, F., T. Tobie and K. Stahl. "Influence of Low Temperatures on Material Properties and Tooth Root Bending Strength of Case Hardened Gears," ASME (Hg.), 2015 — *ASME 2015 International Design Engineering.*
20. Bretl, N., S. Schurer, T. Tobie, K. Stahl and B.-R. Höhn. "Investigations on Tooth Root Bending Strength of Case Hardened Gears in the Range of High Cycle Fatigue," *American Gear Manufacturers Association Fall Technical Meeting,* 2013, pp. 103–118, 2013.

For more information.

Questions or comments regarding this paper?
Contact Thomas Tobie — *tobie@fzg.mw.tum.de.*

Daniel Fuchs studied (2011–2016) at: Ostbayerische Technische Hochschule Regensburg (OTH Regensburg), Germany. Since 2016 he has served as a research associate at the Institute of Machine Elements — Gear Research Centre (FZG) of the Technical University of Munich. Fuchs' expertise is in the influence of non-metallic inclusions on the tooth root load carrying capacity of gears and the influence of coarse grain on the load carrying capacity of gears.

Stefan Schurer has since 2016 worked in the department for technology development of gear parts at MAN Truck & Bus AG, Munich. From 2010–2015 he was a research associate at the Institute of Machine Elements — Gear Research Centre (FZG) of the Technical University of Munich.

Dr.-Ing. Thomas Tobie studied mechanical engineering at the Technical University of Munich (TUM), Germany. Today he is head of the Load Carrying Capacity of Cylindrical Gears department at the Gear Research Centre (FZG), where he specializes in gear materials, heat treatment, gear lubricants and gear load carrying capacity research. Concurrently, Tobie brings to that work a particular focus on all relevant gear failure modes such as tooth root breakage, pitting, micropitting and wear, as well as sub-surface-initiated fatigue failures.

Prof. Dr. Karsten Stahl is Chair, Machine Elements, Mechanical Engineering, at TUM. He leads and conducts research in the area of mechanical drive systems, with particular interest in investigating the load capacity, efficiency and dynamics of all gears types. His other areas of interest include applications in automotive engineering such as synchronization systems and multi-disc clutches. Stahl has developed methods for analysis that have been incorporated into international standards, together with the component strength values derived by means of these methods. He studied mechanical engineering at TUM and performed his doctoral studies from 1994 to 2000 in the Machine Elements Department. In 2001, he joined BMW, first as a gear development engineer, then as the manager of gear development in Dingolfing. In 2006 he transferred to the MINI plant in Oxford where he was initially quality manager for transmissions, then quality manager for powertrains and suspensions. In 2009 he took over responsibility for the initial development and innovation management of powertrain and vehicle dynamics systems at BMW in Munich. Stahl has been a full professor in the Machine Elements Department since 2011.